Coherent Raman laser from an Alkali dimer pumped by a frequency comb

Avi Pe'er* and Igal Aharonovich†
Bar-Ilan University, Ramat-Gan, Israel

A novel theoretical model for a coherent Raman oscillator in an Alkali molecular dimer gas is presented, in which the gas in a heat-pipe placed in an optical cavity, is periodically pumped from the ground vibrational state by a matched frequency comb. Spontaneous emission of the excited wave-packet to different vibrational states in the ground electronic potential is then accumulated in the cavity, and synchronized with the following frequency comb pulses, producing a stimulated Raman transition. Simulation studies show that near the oscillation threshold, the accumulated radiation develops into a train of pulses, which can efficiently dump the excited wave packet into an almost pure single non-zero ground vibrational state. The train of pulses carries the signature of the excited wave packet dynamics.

This technique, therefore, may be useful both for studying of molecular properties and dynamics, as well as aid in achieving quantum coherence control.

Measuring vibrational dynamics in molecules can benefit in achieving a long sought goal of quantum coherence control, namely, steering chemical reactions to do a desired task, while suppressing competing processes [22, 23, 27]. Measurement of vibrational dynamics to date is based either on pump-probe configuration or on wave-packet tomography. In pump-probe, a strong pump pulse excites the dynamics, and a delayed probe pulse probes it, usually by selectively ionizing or dissociating the molecule depending on the vibrational state, measuring the emitted electron or ion [11]. In wave-packet tomography, spontaneous emission from a molecule is measured in a time resolved manner, allowing observation of the time-dependent fluorescence from the vibrating wave-packet due to time-dependent Franck-Condon overlap between the wave-packet and the ground state [30, 31]. Both methods are inherently limited by the small measured signal per molecule (less than one photon/electron). Thus, both methods are inherently slow and require considerable averaging to obtain a desirable signal-to-noise ratio, either over a large ensemble of molecules, or, in time, over many pump pulses. Averaging is essentially *incoherent* accumulation of the light *intensity* from many molecules.

Here, an alternative method is presented, in which the optical signal per molecule is amplified using a coherent cavity amplifier for the spontaneous emission from molecules. When the excitation pulse is repeated synchronously with the cavity round trip (tooth-to-tooth comb excitation), the emission after one pump returns to the molecular medium together with the next pump pulse, allowing stimulated amplification of the originally spontaneous molecular emission. It will be argued here that indeed, it is possible to cross the oscillation threshold with this coherent amplifier and produce a coherent-Raman oscillator, pumped by a frequency comb, which will effectively increase by orders of magnitude, the number of photons emitted per molecule.

The method described here is based on previous works of one of us [16, 21, 26], in which concepts of direct control of molecular dynamics were described. Specifically, a method for coherent transfer of population to a designated vibrational molecular target state with near unity efficiency was shown, using a coherent train of weak pump-dump pulse pairs and a vibrational wave packet as an intermediate [16, 21]. In the system proposed here, the coherent memory is switched from the molecules to the accumulated field, although the logic of the coherent accumulation is essentially identical, and the theoretical technique is equivalent on both analytic analysis and numerical simulation of the molecular dynamics.

It is important to note here the difference between the current proposal and common methods of Raman spectroscopy [4, 14], such as Raman fluorescence spectroscopy, stimulated Raman spectroscopy (SRS) [6, 20] and coherent anti-Stokes Raman spectroscopy (CARS) [5, 17, 29] (where just recently important contributions were made using two frequency combs [2, 8]). All those well-established methods measure molecular vibrational levels *in the ground electronic potential*, and therefore, the pump field is tuned *away from all absorption bands* to ensure a purely *virtual* Raman transition between ground levels. In contrast, the method described here aims to observe the vibrational dynamics *in the excited electronic potential*, and therefore, the pump pulses are tuned *to the molecular absorption* band in order to excite a meaningful wave-packet. In addition, the dump pulse here is not set externally, but rather amplified from spontaneous emission through coherent accumulation and is subject to mode-competition in the laser cavity. The final state of the Raman transfer is not known a-priori, as it is selected by oscillator dynamics, it can either be a single vibrational state or a wave packet, as shown by the simulations below.

The conceptual layout of the system is outlined in figure 1, and a simplified illustration of the underlying molecular excitation progression, for the K_2 dimer, is shown in figure 2. Whenever a pump pulse traverses the molecular medium, a vibrational wave-packet is launched on the excited electronic potential, which dynamics is the

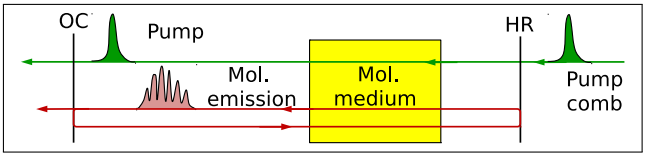

FIG. 1: The conceptual operation of the apparatus , where the pump pulse is followed by a coherent stimulated emission due to interaction with the recurring accumulated emission from previous pulses.

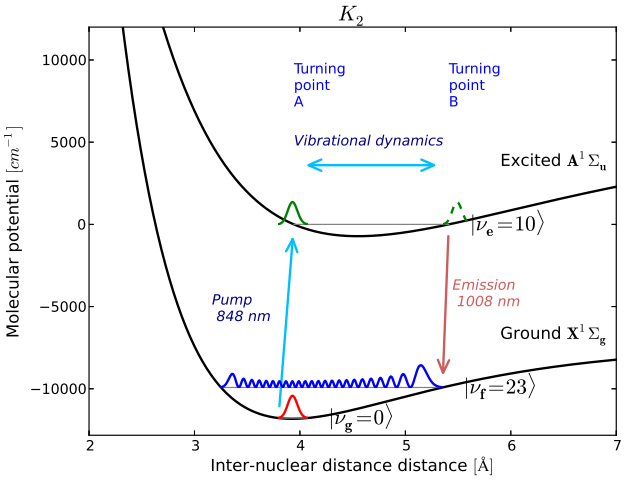

FIG. 2: Vibrational dynamics scheme for K_2 Alkali dimer.

target of our measurement. As the wave-packet vibrates and disperses in the excited potential, emission occurs primarily when the wave packet passes the turning point B, where transition is most effective, in this case, to the vicinity of the state $\nu_e = 23$.

The system is arranged such that the excitation pump comb is locked to the cavity repetition rate. Therefore, the molecular emission from one pulse returns to the medium synchronously with the next pump pulse, enabling coherent accumulation and amplification by stimulated emission. The cavity (and the comb) repetition rates are low enough, such that all molecules decay back to the ground vibrational mode before the next pump pulse arrives. In other words, the coherent memory lingers only in the accumulated light, whereas the molecules themselves begin each pulse a new from the same ground state, with no memory of previous pulses. For an oscillation above threshold, the possible decay channels will compete for pump resources, pushing the oscillation towards one winning channel. Shaping of the pump spectral amplitude and phase can affect the temporal overlap of the wave-packet with a specific target state, thereby providing a mechanism to steer the mode competition towards the desired winner.

The emitted field from the molecular medium in the cavity is calculated within the dipole approximation. Assuming a molecular dipole moment $\boldsymbol{P}(t) = P(t)\hat{\boldsymbol{\mu}}$ where $P(t)$ is a scalar that varies with time and $\hat{\boldsymbol{\mu}}$ is a unit vector in the direction of the dipole, which we take as perpendicular to the optical axis $\hat{\boldsymbol{z}}$. Thus dipole emitted field simplifies to (cf. [3, 9] for full expression):

$$E(z,t) = \frac{1}{4\pi\varepsilon_0 c^2}\frac{\mathrm{d}^2}{\mathrm{d}t^2}P(t - r/c) \tag{1}$$

In a large molecular ensemble, the emitted field can be calculated assuming all molecular dipoles oscillate with the quantum average dipole moment

$$\begin{aligned} P(t) &= e^{-i\omega t} e\mu_{eg} \left\langle \psi_g^{(v)}(t) | \psi_e^{(v)}(t) \right\rangle + c.c. \\ &\equiv p(t)e^{-i\omega t} + \text{c.c.} \end{aligned} \tag{2}$$

where $|\psi_{g,e}^{(v)}(t)\rangle$ are the vibrational state functions of the ground and excited electronic states, $\mu_{eg} = \bar{\mu}_{ge} \equiv \mu$ is the electronic dipole moment between the potentials, assumed to be independent of the inter-nuclear distance. $|\psi_e^{(v)}(t)\rangle$ is viewed from the rotating frame at frequency ω and $p(t)$ is the corresponding rotated dipole amplitude, which reflects the time-dependent Franck-Condon overlap between the ground and excited wave-functions. According to equation 1, the dipole emission from the molecules is proportional to the 2$^{\text{nd}}$ time-derivative of the average dipole $P(t)$:

$$\frac{\mathrm{d}^2}{\mathrm{d}t^2}P(t) \approx [-\omega^2 p(t) - 2i\omega\dot{p}(t)]e^{-i\omega t} + \text{c.c.} \tag{3}$$

For this purpose, we solve the vibrational Schrödinger equations on the coupled potentials

$$i\hbar\frac{\mathrm{d}}{\mathrm{d}t}\begin{pmatrix}\psi_g \\ \psi_e\end{pmatrix} = \begin{pmatrix} T_N + U_g(R) & -\mu E(t) \\ -\mu\bar{E}(t) & T_N + U_e(R) - \hbar\omega \end{pmatrix}\begin{pmatrix}\psi_g \\ \psi_e\end{pmatrix} \tag{4}$$

where R is the inter-nucleic distance, $T_N = -\hbar^2/(2M)\partial^2/\partial R^2$ is the kinetic energy operator of the nuclei, M is the reduced mass, $U_{e,g}(R)$ is the ground/excited potential curve and $E(t)$ is the slow varying amplitude of the accumulated field. From (4) and (2) we find

$$\frac{\hbar}{i}\frac{\dot{p}(t)}{e\mu} = \langle\psi_g| U(R) |\psi_e\rangle + \mu E(t)\left[|\psi_g|^2 - |\psi_e|^2\right] \tag{5}$$

where $U(R) \equiv U_e(R) - U_g(R)$ is the electronic energy difference of order $\hbar\omega$. The microscopic *emitted* field $E(z,t)$ can is then calculated using (5), (3) and (1). Note that (5) contains contributions both from the ground-excited superposition and the *stimulated emission* proportional to the time-dependent population inversion between the target state and the wave-packet in the excited potential

surface, and thus, forms a coherent wave-packet generalization of the well-known rate equations of standard lasers [25].

Specifically, each pulse was simulated starting with the same initial conditions of the molecular matter in the ground vibrational state, where it encounters the same pump pulse and the intra-cavity field accumulated up to the current iteration. The Scrödinger equation (4) was then solved numerically using the split operator method [7] to obtain the vibrational time-dependent wave functions $|\psi_{e,g}(R,t)\rangle$. With these, the *microscopic* emitted field per molecule can be calculated using (5), (3) and (1). The *macroscopic* field is then evaluated, by the method shown below, and then added coherently to the already existing field to produce the intra-cavity drive field for the next iteration (with appropriate decoherence, decay and dispersion). To account for spontaneous emission, a white noise of the order of one-photon in amplitude, is also added to the accumulated intra-cavity in every iteration (in fact, this was the seed of the first emission). The long time between pump pulses is assumed long enough for the molecules to decay completely to the vibrational ground state, which is reasonable for a hot, pressure broadened molecular ensemble.

The macroscopic field gain can be calculated considering the following assumptions: a) the collection of molecules radiate coherently as a single excited macroscopic dipole if observed far enough. It then decays on a time scale given by T_2, as dictated by collisions and other broadening mechanisms in the medium. b) the accumulated inducing field is Gaussian beam in space, which corresponds to TEM_{00} mode of the laser cavity and is matched to the pump spatial mode as well. c) there is a linear relation, at any position $\boldsymbol{r}$ in the ensemble gas, between the induced dipole moment (and its second derivative), and the inducing field at this point (a common assumption for stimulated emission, also verified by the simulation). Consequently, the spatial mode of the emitted field is inherently the same Gaussian mode of the inducing field. d) As a direct result of Fresnel diffraction in the far field, the macroscopic field on the optical axis $E_M^{em}(z)$ at a large enough distance from the beam waist $z \gg z_R$ (the Rayleigh range), is just the coherent summation of all the microscopic dipole contributions $E_M^{em}(z) = nV_{\mathrm{eff}}E_{\mathrm{single}}^{em}(z)$, where n is the molecular density and V_{eff} is the effective illuminated volume.

We then assume the molecular medium is placed at the waist of the cavity mode and calculate the emitted field at a distance $z = 20z_R$, well within the far-field range. According to Fresnel diffraction, this on-axis field is the peak value of the emitted Gaussian spatial mode, which is identical to the inducing Gaussian mode. We can thus use Gaussian optics to propagate the emitted field back to the waist, where it is added to the inducing field in preparation for the next iteration. The macroscopic single-pass gain is thus expressed based on the microscopic emission extracted from the simulation.

The oscillation threshold can now be immediately estimated from the calculated gain and the assumed cavity losses. Our simulation showed that for a gain medium of K_2 molecules in a cavity with 5% linear losses is pumped by a 1W average power comb source at 100MHz repetition rate (10 nJ/pulse), the threshold density is 10^{12}molecules/cm^3 at an interaction length of 10 cm, which is convenient to achieve in a heat-pipe experiment. The decoherence window assumed in the simulation was of the order of $T_2 \approx 35$ ps, which seems conservative for the relevant temperature and pressure conditions. The threshold density for Rb_2 dimers was very similar, whereas for Li_2 it was slightly higher (10^{13}molecules/cm^3) due to the lower transition dipole-moment of Li_2 compared to K_2.

Extensive simulations of the coherent Raman oscillator were made with three candidate Alkali dimers - Li_2, K_2 and Rb_2. As electronic potential curves we used spectroscopic data from the literature (Morse potential fits) [10, 13, 15] for the ground $X^1\Sigma_g$ and excited $A^1\Sigma_u$ states. For the transition dipole moments we assumed the atomic values of the D-line, neglecting spin-orbit effects. In figure 3, snapshots of the intra-cavity response (cavity field and the molecular populations) immediately after a pump pulse excitation, where the Raman oscillator is pumped slightly above threshold (a few percent). The snapshots are taken at two stages of the dynamics - during cavity buildup, when population depletion from the excited wave packet is unobserved yet; and at a steady state, after the mode competition has settled down. The figure shows the intra-cavity field (1$^{\mathrm{st}}$ row), excited wave packet population and target state population (2$^{\mathrm{nd}}$ row) and the vibrational purity of the target state (the fraction of the final state population that occupies a single vibrational level, 3$^{\mathrm{rd}}$ row).

The results show the following features: (a) Complete damping of the excited wave packet to the target state is obtained, even though the oscillator is pumped only a few percent above threshold. This is in complete contrast to standard lasers, where the excited state population clamps to the threshold value, and can never be completely dumped. Thus, this Raman oscillator shows ideal photon efficiency (one emitted photon per every pump photon absorbed). (b) Near threshold, the emitted field forms a long train of pulses matched to the excited wave packet vibrations. However, the main emission does not appear immediately after the pump, but rather takes nearly 30ps to develop. At first, this can be surprising as the simulation's coherence decay window is set at $T_2 = 35$ps. (c) As the pump is increased above threshold, the emitted pulse train becomes shorter, and appears at an earlier time after the pump pulse, up to a very high pump where the emission takes the form of a single primary pulse, that dumps most of the population immediately after the pump pulse. (d) Conversely, as

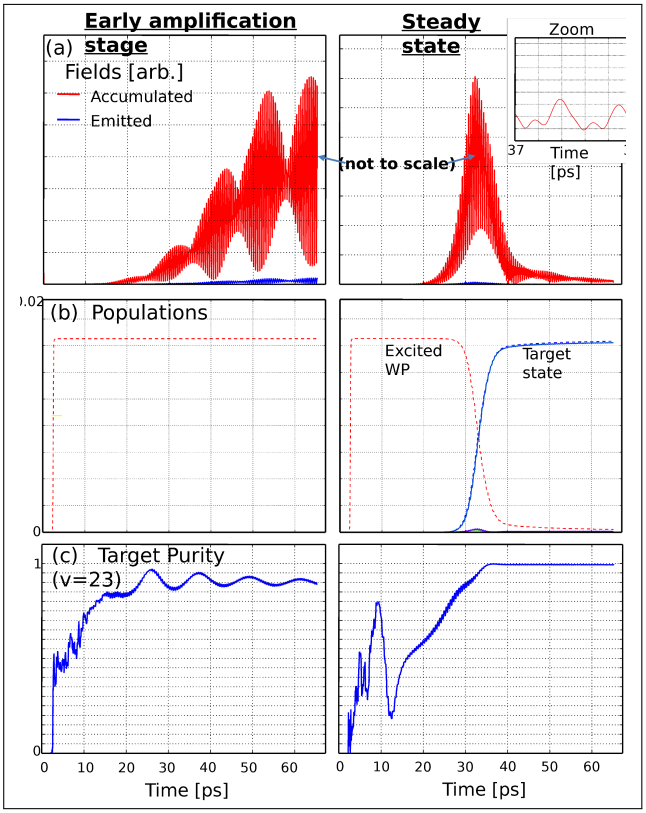

FIG. 3: Simulation results slightly above threshold for K_2. Left column shows results of a given pulse at an earlier stage, and the right column shows the type of results at a stable oscillation stage. In the first row, the emitted (blue) and accumulated (red) fields are shown. The rapid oscillation is due to the vibrational dynamics. In the second row, population of the excited (red) and target (blue) potential curves are shown. In the lower row, the purity of the target state with regard to the specific vibrational state $|\nu = 23\rangle$ is shown.

the pump is reduced towards threshold, the main group of oscillations is pushed towards longer times, until eventually suppressed by the decoherence window ($T_2 = 35$ps in this simulation) and can no longer coherently dump all the excited population to the target state. *The threshold for coherent oscillation is therefore a direct result of the available coherence time*, and if longer coherence were available, the threshold would be reduced (as indeed seen in the simulations). (e) A high vibrational purity of the target state is achieved near threshold. For Li_2, practically all the dumped population occupies a single vibrational state ($> 99.99\%$), and this purity is achieved rather early in time, even before the main bulk of the population is actually transferred. For K_2 the purity is a little lower at $> 98\%$, and for Rb_2 the purity was $> 90\%$. These high purities are achieved autonomously by the system due to the physical preference in the mode competition stage, and will be discussed further below. (f) At high above threshold, the emitted field shortens in time and the purity of the target state is lower (though for Li_2 purity is much more robust due to its faster dynamics).

The Raman oscillator behaves as ordinary laser in the sense that it seeks to dump the excited population in an efficient way. However, the coherent radiation can be used the dump the entire excited population over a longer time, and thus with higher efficiency, just like in a simple two level system, where energy required for a π-pulse is inversely proportional to its duration. Thus, near threshold, where the available energy for the dump is low, a long coherent train (as long as the decoherence allows) develops. As the pump is increased above threshold, the available dump energy increases, and the population can be dumped faster.

The high purity is the result of the different vibrational periods of the excited and target potential curves, where the large duration of transfer $\tau_{\rm dyn} > 1/(\nu_e - \nu_f)$, where $\nu_e - \nu_f$ is the difference between the vibrational periods (in terms of frequency), and therefore, transfer occurs only to a single state. As long as the *actual* coherence time $T_2 > 1/(\nu_e - \nu_f)$, high purity can be achieved for K_2 and Rb_2 as well (which are heavier and consequently shows slower vibrational dynamics).

In order to estimate the coherence time, we use the molecular dimer threshold density derived in the simulation, and since the molecules are produced in a hot Alkali vapor cell, where dimers constitute $0.5 - 1\%$ of the density [28], the major factor for T_2 would be collisions with the surrounding atoms. For dimer densities of 10^{12-13} molecules/cm^3, the atomic density needs to reach 10^{14-15} atoms/cm^3, which maps to a temperature range of $470^\circ - 550^\circ K$. Even at higher atomic pressures of 10^{15} atoms/cm^3, the corresponding vapor pressure in the cell is at most of 1 Torr [1]. The exact pressure broadening of $K - K_2$ is not known to us, however, the atomic pressure broadening ($K - K$ collisions) of the D_1 line is $2GHz$/Torr [24]. This is an anomalously high value, since it is affected by resonant dipole-dipole collisions which have large cross-sections. For non-resonant collisions, typical broadening values are of a few $10-100MHz$ [12, 18, 19]. For K_2, the molecular transitions are far detuned from the atomic lines, and therefore, the $K - K_2$ collisions are expected to be predominantly non-resonant. Yet, even if we adopt the severe atomic broadening value, the collisional coherence is expected to be > 100ps, which is more than sufficient for the coherent Raman oscillator. Other sources of broadening such as Doppler are not expected to be an important factor in T_2 (Doppler broadening, for instance, nearly cancels out in Raman transitions).

Thus, the coherent Raman oscillator presented here seems to be realizable, showing both novel coherence and selectivity features, offering avenues for exploring molecular properties and dynamics even beyond the Alkali dimers presented here.

* avi.peer@biu.ac.il
† jigal2@gmail.com

[1] C. B. Alcock, V. P. Itkin, and M. K. Horrigan. Vapour Pressure Equations for the Metallic Elements: 298–2500K. *Canadian Metallurgical Quarterly*, 23(3):309–313, 1984-07-01T00:00:00.

[2] Birgitta Bernhardt, Akira Ozawa, Patrick Jacquet, Marion Jacquey, Yohei Kobayashi, Thomas Udem, Ronald Holzwarth, Guy Guelachvili, Theodor W. Hansch, and Nathalie Picque. Cavity-enhanced dual-comb spectroscopy. *Nat Photon*, 4(1):55–57, Jan 2010.

[3] Max Born and Emil Wolf. *Principles of Optics: Electromagnetic Theory of Propagation, Interference and Diffraction of Light (7th Edition)*. Cambridge University Press, 7th edition, 1999.

[4] Ji-Xin Cheng and Xiaoliang Sunney Xie. *Coherent Raman Scattering Microscopy*. Series in Cellular and Clinical Imaging . CRC Press, 2012.

[5] Nirit Dudovich, Dan Oron, and Yaron Silberberg. Single-pulse coherently controlled nonlinear Raman spectroscopy and microscopy. *Nature*, 418(6897):512–514, Aug 2002.

[6] Christian W. Freudiger, Wei Min, Gary R. Holtom, Bingwei Xu, Marcos Dantus, and Sunney XieX. Highly specific label-free molecular imaging with spectrally tailored excitation-stimulated Raman scattering (STE-SRS) microscopy. *Nat Photon*, 5(2):103–109, Feb 2011.

[7] B M Garraway and K A Suominen. Wave-packet dynamics: new physics and chemistry in femto-time. *Reports on Progress in Physics*, 58(4):365, 1995.

[8] Takuro Ideguchi, Simon Holzner, Birgitta Bernhardt, Guy Guelachvili, Nathalie Picque, and Theodor W. Hansch. Coherent Raman spectro-imaging with laser frequency combs. *Nature*, 502(7471):355–358, Oct 2013. Letter.

[9] John David Jackson. *Classical electrodynamics*. Wiley, New York, NY, 3rd ed. edition, 1999.

[10] P. Jasik and J.E. Sienkiewicz. Calculation of adiabatic potentials of Li2. *Chemical Physics*, 323(2–3):563–573, 2006.

[11] Hiroyuki Katsuki, Hisashi Chiba, Bertrand Girard, Christoph Meier, and Kenji Ohmori. Visualizing Picometric Quantum Ripples of Ultrafast Wave-Packet Interference. *Science*, 311(5767):1589–1592, 2006.

[12] Kotusingh Lulla, Howard Howland Brown, and Benjamin Bederson. Total Cross Sections for the Scattering of Potassium by He, Ne, Ar, Xe, and H_2 in the Thermal Energy Range. *Phys. Rev.*, 136:A1233–A1239, Nov 1964.

[13] S. Magnier and Ph. Millié. Potential curves for the ground and numerous highly excited electronic states of K_2 and NaK. *Phys. Rev. A*, 54:204–218, Jul 1996.

[14] Laurence A. Nafie. Recent advances in linear and nonlinear Raman spectroscopy. Part VI. *Journal of Raman Spectroscopy*, 43(12):1845–1863, 2012.

[15] Su Jin Park, Sung Won Suh, Yoon Sup Lee, and Gwang-Hi Jeung. Theoretical Study of the Electronic States of the Rb2 Molecule. *Journal of Molecular Spectroscopy*, 207(2):129–135, 2001.

[16] Avi Pe'er, Evgeny A. Shapiro, Matthew C. Stowe, Moshe Shapiro, and Jun Ye. Precise Control of Molecular Dynamics with a Femtosecond Frequency Comb. *Phys. Rev. Lett.*, 98:113004, Mar 2007.

[17] John Paul Pezacki, Jessie A. Blake, Dana C. Danielson, David C. Kennedy, Rodney K. Lyn, and Ragunath Singaravelu. Chemical contrast for imaging living systems: molecular vibrations drive CARS microscopy. *Nat Chem Biol*, 7(3):137–145, Mar 2011.

[18] Greg A. Pitz, Andrew J. Sandoval, Nathan D. Zameroski, Wade L. Klennert, and David A. Hostutler. Pressure broadening and shift of the potassium {D1} transition by the noble gases and N2, H2, HD, D2, CH4, C2H6, C3H8, and n-C4H10 with comparison to other alkali rates. *Journal of Quantitative Spectroscopy and Radiative Transfer*, 113(5):387–395, 2012.

[19] Paul Rosenberg. Collision Cross Sections of K Atoms and K_2 Molecules in Gases. *Phys. Rev.*, 55:1267–1267, Jun 1939.

[20] Brian G. Saar, Christian W. Freudiger, Jay Reichman, C. Michael Stanley, Gary R. Holtom, and X. Sunney Xie. Video-Rate Molecular Imaging in Vivo with Stimulated Raman Scattering. *Science*, 330(6009):1368–1370, 2010.

[21] Evgeny A. Shapiro, Avi Pe'er, Jun Ye, and Moshe Shapiro. Piecewise Adiabatic Population Transfer in a Molecule via a Wave Packet. *Phys. Rev. Lett.*, 101:023601, Jul 2008.

[22] Moshe Shapiro and Paul Brumer. Laser control of product quantum state populations in unimolecular reactions. *The Journal of Chemical Physics*, 84(7):4103–4104, 1986.

[23] Moshe Shapiro and Paul Brumer. Coherent control of molecular dynamics. *Reports on Progress in Physics*, 66(6):859, 2003.

[24] A. Siegman. *Lasers*. University Science Books, 1st edition edition, May 1986.

[25] Anthony E. Siegman. *Lasers*. University Science Books, 1986.

[26] Matthew C. Stowe, Michael J. Thorpe, Avi Pe'er, Jun Ye, Jason E. Stalnaker, Vladislav Gerginov, and Scott A. Diddams. Direct frequency comb spectroscopy. In Paul R. Berman Ennio Arimondo and Chun C. Lin, editors, , volume 55 of *Advances In Atomic, Molecular, and Optical Physics*, pages 1–60. Academic Press, 2008.

[27] David J. Tannor and Stuart A. Rice. Control of selectivity of chemical reaction via control of wave packet evolution. *The Journal of Chemical Physics*, 83(10):5013–5018, 1985.

[28] A F J van Raan, J E M Haverkort, B L Mehta, and J Korving. Two-step photoexcitation of K 2 molecular Rydberg states in a heat-pipe oven. *Journal of Physics B: Atomic and Molecular Physics*, 15(18):L669, 1982.

[29] Andreas Volkmer, Lewis D. Book, and X. Sunney Xie. Time-resolved coherent anti-Stokes Raman scattering microscopy: Imaging based on Raman free induction decay. *Applied Physics Letters*, 80(9):1505–1507, 2002.

[30] Ian A Walmsley and Leon Waxer. Emission tomography for quantum state measurement in matter. *Journal of Physics B: Atomic, Molecular and Optical Physics*, 31(9):1825, 1998.

[31] Ian.A. Walmsley, ThomasJ. Dunn, and JohnN. Sweetser. Characterizing the Quantum State of Matter Using Emission Tomography. In JosephH. Eberly, Leonard Mandel, and Emil Wolf, editors, *Coherence and Quantum Optics VII*, pages 73–82. Springer US.